here; for, although we have considered a complex plane of orderings in the procedure of Sec. VI, there exists a considerable variety of other types of ordering. The three ways of ordering the operators p and q considered in Sec. IV of I, for example, are easily generalized to a complex plane of q, p orderings.

If, however, the relation (10.13) should apply to the s-ordered products for some value of s, then, by forming the ensemble average of the series (2.7) for $D(\xi,s)$, we would obtain the relation

$$\chi(\xi,s)=\int e^{\xi\alpha^*-\alpha^*\xi}w(\alpha)\pi^{-1}d^2\alpha\,, \qquad (10.14)$$

which upon Fourier inversion would imply $w(\alpha)=W(\alpha,s)$.

PHYSICAL REVIEW VOLUME 177, NUMBER 5 25 JANUARY 1969

Nuclear Interactions and Cosmic Radiation at Energies around 10^6 GeV

C. B. A. McCusker, L. S. Peak, and M. H. Rathgeber
Cornell-Sydney University Astronomy Center, The University of Sydney, Sydney, N. S. W., Australia
(Received 3 June 1968)

The results of a series of Monte Carlo simulations of extensive air showers are compared with experimental data from the Sydney 64-scintillator array and other experiments. The work has had two main objectives: (a) the study of the composition of cosmic radiation around 10^6 GeV; (b) the study of nuclear interactions at very high energies. In the first field, evidence is produced to show that the composition of cosmic radiation is much the same at 10^{15} eV total energy as at 5×10^{10} eV total energy. Above about 3×10^{15} eV the composition changes, the beam becoming progressively richer in heavier nuclei up to energies of about 10^{17} eV. In the second field, the main result reported is that at energies above 10^{14} eV there is evidence that much higher transverse momenta occur than at machine energies. If true, this implies that a force is acting which is much stronger than the normal strong interaction.

1. INTRODUCTION

VERY high-energy nuclear interactions can only be studied using the cosmic radiation. Up to energies of $\sim2\times10^{14}$ eV, occasional interactions in very large emulsion stacks can be found. Above that energy the events become too rare for this method, and then air-shower techniques (sometimes involving emulsions) must be used. Several recent experiments[1] have suggested that new fundamental processes may become important above 10^{14} eV; hence it is more important than ever to study this region. In particular, we wish to know the composition of the radiation and how it varies with energy, both because this would make our study of the fundamental interactions easier and also because it is of considerable interest to astrophysicists. In recent years considerable progress has been made experimentally. We can now study the core region of air showers in considerable detail. Until recently, however, progress was hindered because the mathematical methods available were not able to relate these detailed properties of the fundamental parameters of the basic nuclear reactions and the nature of the primary particle. However, this is no longer so. With the improvement in speed and storage capacity of modern computers it has become possible to calculate quite fine details in air-shower core structure and so on from the fundamental parameters using Monte Carlo techniques. In this paper we report the results of such calculations using four different primary particles (with $A=1$, 4, 16, and 64), eight different models of the fundamental nuclear interaction, and three different primary energies. These theoretical calculations are then compared with the results of experiments at Sydney and elsewhere.

We conclude that there is good evidence for the occurrence of very high transverse momenta in nuclear interactions at energies $\gtrsim10^{14}$ eV and that this implies the existence of some very strong force; that the composition of the cosmic ray beam is roughly constant up to about 2×10^{15} eV; and that from this energy up to about 10^{17} eV it becomes progressively richer in heavier nuclei.

2. SIMULATION PROCESS

In the simulation process we supposed that incident particles of atomic weight A and energy E_p were incident vertically on an exponential atmosphere and aimed at the center of a 9×9 array of scintillators. Each scintillator measured 0.5×0.5 m, and they were in contact. The position in the atmosphere of each interaction of all hadrons was sampled by the Monte Carlo technique from a distribution giving a mean free path of λ g/cm^2. The numerical value of λ was 90 g/cm^2 for protons and pions, and 65, 43, and 42 g/cm^2, respec-

* Work supported by the Science Foundation for Physics of the University of Sydney, and by the U. S. Air Force Office of Scientific Research under Grant No. AF-AFOSR-676-66.
[1] C. B. A. McCusker, Can. J. Phys. 46, 397 (1968).

TABLE I. Parameters used in different models. γ^* is the Lorentz γ of the fireball in the center-of-momentum system.

Model name	p_1	p_2	p_3	p_4	He1	O1	Cu1	He4
Atomic weight of primary	1	1	1	1	4	16	64	4
Mean free path of primary in g/cm^2	90	90	90	90	65	43	42	65
Mean multiplicity of pions proportional to	$\ln E$	$E^{1/4}$	$E^{1/4}$	$\ln E$	$\ln E$	$\ln E$	$\ln E$	$\ln E$
Sampled γ^*	Yes	Yes	No	No	Yes	Yes	Yes	Yes
Fireball's fraction of incident energy	$\sim$0.5	$\sim$0.5	0.5 fixed	0.25 fixed	$\sim$0.5	$\sim$0.5	$\sim$0.5	$\sim$0.5
Isobar decay pions fraction of incident energy	None	None	None	$\sim$0.25	None	None	None	None
Mean transverse momentum of isobar or nucleon in GeV/c	1.0	1.0	1.0	1.0	1.0	1.0	1.0	See text

tively, for α particles, oxygen nuclei, and copper nuclei.

All interactions were considered to be nucleon-nucleon or pion-nucleon collisions (with the exception of the initial interaction of a heavy primary). In all cases, two fireballs were produced with mean secondary multiplicities proportional to $\ln E$ or to $E^{1/4}$ and Poissonian distribution. The type of secondary was chosen at random with a probability of 0.6 for charged pions, 0.3 for neutral pions, and 0.1 for nucleons. The direction of emission was chosen at random in the fireball reference frame, and the momentum was chosen with a mean of 0.5 GeV/c for pions and 1.0 GeV/c for nucleons and distributed like pe^{-p}. The momentum of the last fireball secondary was chosen to make the total momentum zero. The backwards fireball was the mirror image of the forward one. In some models the gamma of the fireball in the c.m. frame (γ^*) was sampled from a pe^{-p} distribution with a mean chosen to make the mean inelasticity$=0.5$. The resulting distribution of inelasticity varied somewhat with energy but was very roughly uniform over the interval 0–1. In other models the inelasticity was fixed and γ^* adjusted to balance energies. In some models the fireballs themselves were given sampled transverse momenta. These will be described in detail later. All secondary pions and nucleons with energies below 50 GeV were discarded.

In all cases, the backward-emerging nucleon or isobar was ignored although they balanced the momentum of their forward-moving counter parts. The forward-energing particle carried away all the remaining energy and, if it was a nucleon, was given a transverse momentum sampled from a pe^{-p} distribution with a mean of 1 GeV/c in most cases. In one model we assumed two isobars to be produced in addition to the fireballs. This model had no secondary nucleons emitted from the fireballs. The isobar mass was taken to be 1.5 GeV. The decay was assumed to be into a single pion and a nucleon with a $\cos^2\theta$ angular distribution in the isobar system, since it is likely for these isobars to have some intrinsic spin. 25% of the total energy went into the fireballs, with the result that on the average $\sim$50% went into the nucleon from the isobar and the remaining 25% went to the isobar pion. This pion had a probability of $\frac{1}{3}$ of being neutral.

Secondary neutral pions decayed immediately into two photons. Charged pions could decay to muons or interact in a similar way to nucleons (possibly with different parameters) and without isobar formation.

For the first interaction of heavy primaries, the impact parameter was sampled at random and determined the number of nucleons actually taking part in nucleon-nucleon collisions in the first interaction. All remaining incoming nucleons were given a transverse momentum individually sampled from pe^{-p} distribution with mean 0.3 GeV/c. Table I gives a summary of the parameters used in the different models.

Nucleons and pions were followed until they decayed or interacted. When neutral pions decayed to two γ rays the direction (in the pion frame of reference) of one of the decay photons was chosen at random, thus determining the energies and directions of both photons. The size and "age" of the resulting electromagnetic cascade from each photon was calculated using the one-dimensional shower theory (in approximation B), while the lateral distribution of the electrons was calculated using the numerical approximation to their theoretical structure function developed by Kamata and Nishimura.[2]

The program calculated the number of electrons striking each scintillator of a 9$\times$9 scintillator grid at five different atmospheric depths, namely, 200, 400, 600, 800, and 1000 g/cm^2. It gave the number and energies of all hadrons (of energy $>$50 GeV) striking the same grids. In addition, it gave the total number of electrons and muons at each of the depths, and various other parameters which will be described when necessary. The mean time to simulate one shower using an English Electric KDF9 was 15 minutes. The KDF9 in this application, is about twice as fast as an IBM 7040. Over 800 showers were simulated.

[2] K. Kamata and J. Nishimura, Progr. Theoret. Phys. (Kyoto) Suppl. 6, 93 (1958).

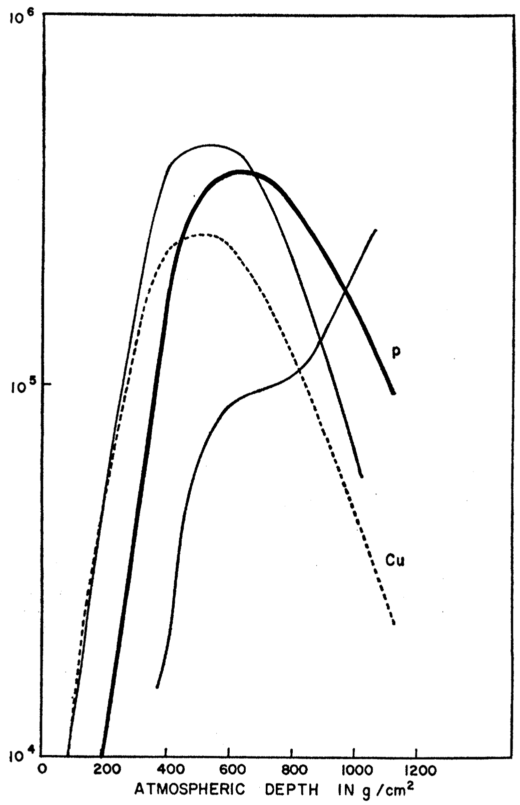

FIG. 1. The average total number of electrons (N_e) in the shower at a given depth in the atmosphere is plotted against the depth for simulated showers initiated by protons (thick solid curve) and by coppper nuclei (dashed curve) of 10^{15} eV total energy. The thin solid curves show the development of the two extreme single showers due to protons.

3. ELECTRON-PHOTON COMPONENT

A. Electron Shower Size

Electrons are the most numerous of the charged particles in air showers. In most experiments to date, the total number of electrons in the shower has been taken to be the measure of the total energy of the primary. Our programs give the electron shower size at five different depths in the atmosphere. Figure 1 shows the way in which the shower size varies on the average with atmospheric depth for proton (p_1) and copper primaries (Cu1) of total energy 10^{15} eV. It also shows the development of the shower for the two most extreme individual showers initiated by protons. The atmospheric depth at which the showers reach their maximum development on the average is 600 g/cm² for the proton-initiated showers and 500 g/cm² for copper-initiated showers. The mean shower sizes at sea level, at 750 g/cm² (Mt. Norikura), and at 530 g/cm² (Mt. Chacaltaya) are given in Table II. One sees that a 10^{15}-eV primary on the average produces a shower four times as large at Mt. Norikura as at sea level. One also notices that the fluctuations for protons

TABLE II. Mean shower sizes at different altitudes for showers initiated by protons or copper nuclei of 10^{15} eV total energy.

	Protons	Copper	Mean
Size at sea level (1030 g/cm²)	5.4×10^4	3.8×10^4	4.6×10^4
Size at 750 g/cm²	2.1×10^5	1.5×10^5	1.8×10^5
Size at 530 g/cm²	3.5×10^5	2.5×10^5	3.0×10^5

can be very considerable. In a sample of 85 showers the extreme sizes at 503 g/cm² were 6.4×10^4 and 4.6×10^5.

B. Number Spectrum

There is another interesting feature to be noted. Suppose that the cosmic-ray energy spectrum for primaries of all different atomic numbers could be represented by a power law of constant exponent up to a given energy per nucleon, at which point it cut off abruptly. Then the number spectrum of air showers would show an almost constant exponent up to a certain value, at which point the slope would begin to increase. The number at which this happened would vary with atmospheric depth, and to a first approximation this number would be given by the mean number of particles in the showers produced by the most energetic primaries. It is, of course, well known that the number spectrum of air showers does show a steepening at a given number and that this number varies with altitude. Table III[3–6] shows some of the experimental results together with the average size of a shower initiated by a 10^{15}-eV proton at the same depths.

TABLE III. The variation with altitude of the point at which the air-shower number spectrum increases its slope ("join point") together with the variation in mean size of showers due to 10^{15}-eV protons.

Depth (g/cm²)	1030	800	620	530
Join point of number spectrum	5×10^5 [a]	2×10^6 [b]	7×10^6 [c]	1.5×10^6 [c]
Size of 10^{15}-eV "proton" shower	1.4×10^5	2.1×10^5	3.7×10^5	3.5×10^5

[a] References 3, 4.
[b] Reference 5.
[c] Reference 6.

[3] C. B. A. McCusker, in *Proceedings of the 1963 Cosmic Ray Conference, Jaipur, India* edited by R. R. Daniel *et al.* (Commercial Printing Press, Ltd., Bombay, India, 1963), Vol. 9, p. 51.

[4] G. T. Zatsepin, S. I. Nikolski, and G. B. Khristiansen, in *Proceedings of the 1963 Cosmic Ray Conference, Jaipur, India,* edited by R. R. Daniel *et al.* (Commercial Printing Press, Ltd., Bombay, India, 1963), Vol. 4, p. 100.

[5] B. K. Chatterjee, G. T. Murthy, S. Naranan, B. V. Sreekantan, and M. V. Srinivasa Rao, in *Proceedings of the 1963 Cosmic Ray Conference, Jaipur, India,* edited by R. R. Daniel *et al.* (Commercial Printing Press, Ltd., Bombay, India, 1963), Vol. 4, p. 227.

[6] G. Clark, H. Bradt, M. LaPointe, V. Domingo, I. Escobar, K. Murami, K. Suga, Y. Toyoda, and J. Hersil, in *Proceedings of the 1963 Cosmic Ray Conference, Jaipur, India,* edited by R. R. Daniel *et al.* (Commercial Printing Press, Ltd., Bombay, India, 1963), Vol. 4, p. 65.

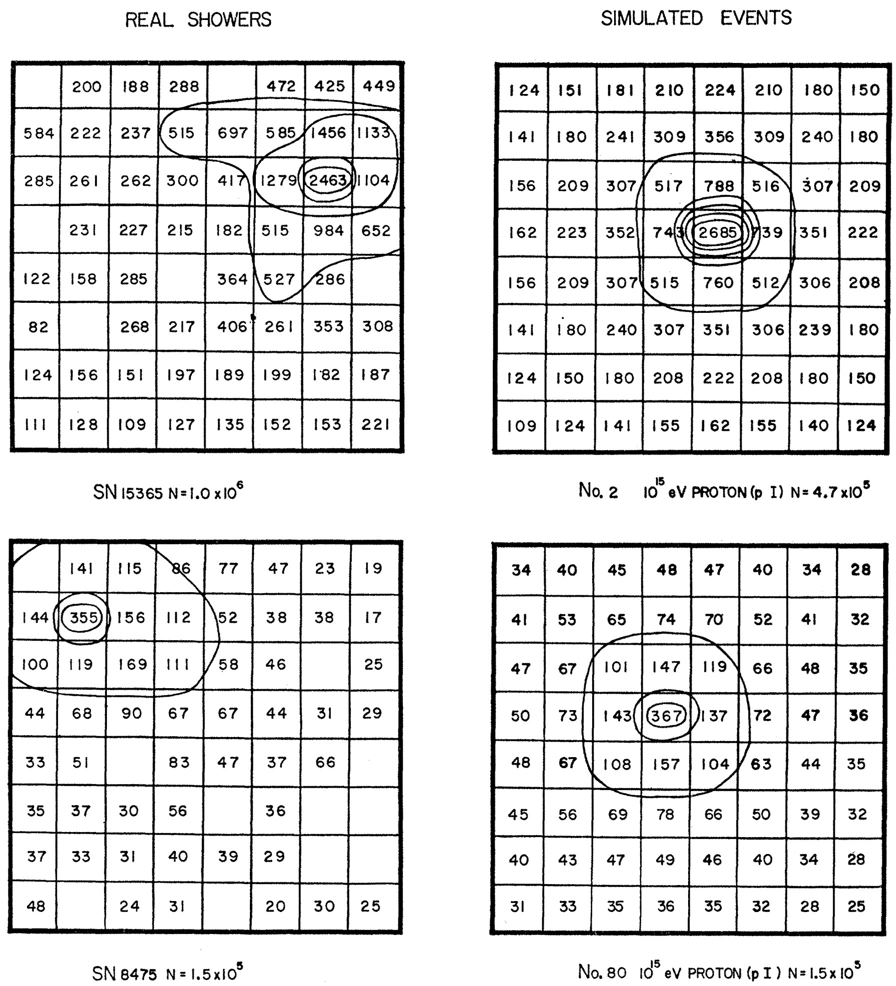

FIG. 2. Four maps of the distribution of electrons on a 4-m $\times$4-m-scintillator array at sea level. Two of the maps are real events detected by the Sydney 64-scintillator array and two are events simulated by the Monte Carlo program for proton primaries of 10^{15} eV. All four events are classed as single-cored showers. For the upper pair contour lines are at density intervals of 500 particles per scintillator; for the lower pair, at 100 particles per scintillator. For real events, a blank means that the scintillator performance on test was substandard.

Experimentally, the determination of the join point of the number spectrum is difficult. The point at which the change of slope takes place is not clearly defined. The statistical errors are large and the apparatus used at the different heights was not standardized. In particular, the array used at El Alto was much larger than at the other altitudes. Nevertheless, it is obvious that the two sets of figures have common features.

C. Electron Core Structure

In addition to the total number of electrons in the shower, our program also gives the distribution of the electrons close to the axis of the shower (± 2.25 m from axis) at the five different altitudes. This allows us to determine the maximum electron density hitting a scintillator in any shower (which we will call Δ_c) and also to classify the cores as "single" or "multiple." In many cases this classification is unambiguous. Figure 2 shows four showers, two of them real and two simulated, which we classify as single-cored events. Four multicored showers are shown in Fig. 3; again two are real and two are simulated.

In a few cases, however, classification is difficult. Accordingly, we have adopted the following objective procedure to define single-cored showers. We take the ratio Δ_{c1}/Δ_{c2} of the density in the most dense scintillator to that in the second most dense. If $\Delta_{c1}/\Delta_{c2} \geqslant 1.5$, we call the shower a single-cored event; if not, a multicored event. We have reclassified all real and simulated events using this definition and find that for 88% of all events we get agreement with our previous "subjective" assignation. A similar system has been adopted by the Osaka group[7] for their experiment on Mt. Norikura. They call single-cored showers those with $\Delta_{c1}/\Delta_{c2} \geqslant 3$. Such an increase is probably necessary to compensate for the difference in altitude.

D. Δ_c-N Diagram

In Fig. 4 we plot Δ_c against the total number of particles N in the shower for showers initiated by four different types of primary (protons, α particles, O

[7] S. Miyake, K. Hinotani, N. Ito, S. Kino, H. Sasaki, H. Yoshii, H. Sakuyama, and E. Kato, Can. J. Phys. (to be published).

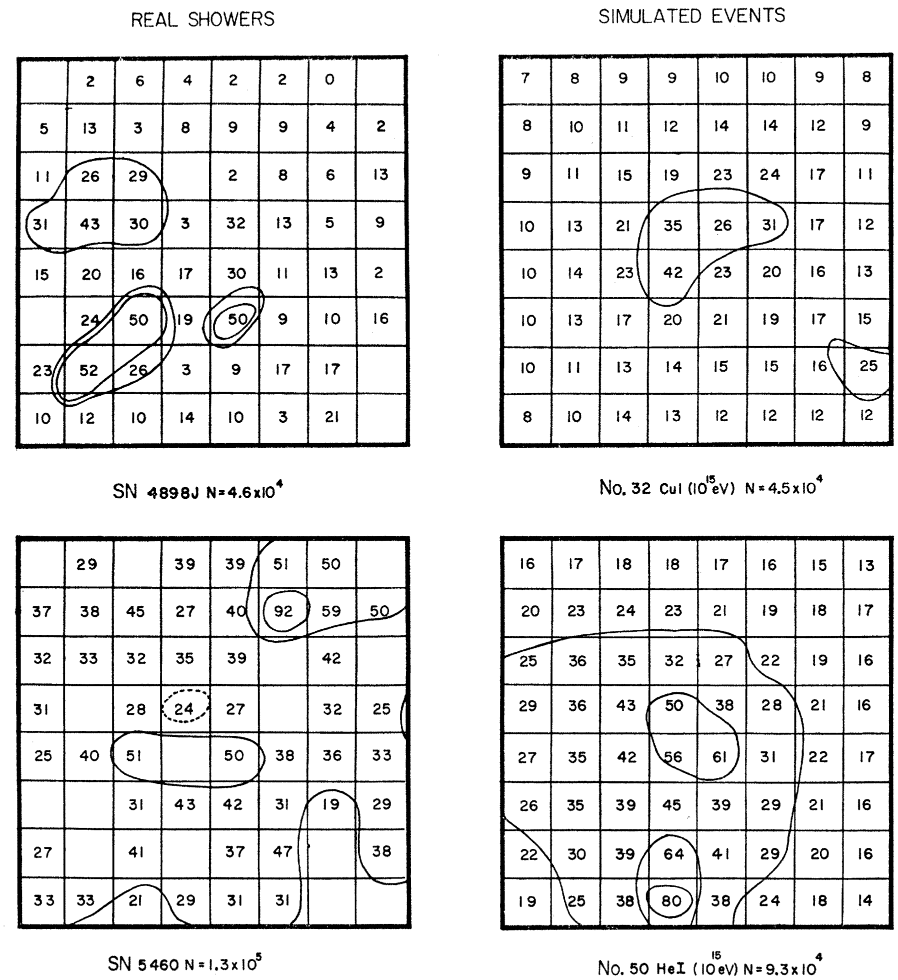

FIG. 3. Four multicored showers. Again, two are real events and two are simulated events assuming a heavy primary of 10^{15} eV total energy. The number in each square is the number of electrons striking that scintillator. Contour lines are at intervals of 25 particles per scintillator. N is the total number of particles in the shower.

nuclei, and Cu nuclei), each of total energy 10^{15} eV. Open figures represent single-cored showers; solid figures, multicored showers. Figure 5 is the same scatter diagram for real air showers whose cores struck the Sydney 64-scintillator experiment from April 1963 to January 1965. The bounding lines of the experimental distribution (labeled p and Fe) have also been drawn on the simulated distribution. No normalization was necessary. The experimental distribution is, of course, for primary particles of many different energies. It can be seen that, while the simulated showers show wide variations in both Δ_c and N, the region they occupy on the diagram is rather limited. At any particular Δ_c, the width of the distribution is only 2.5 to 1. Hence we would get complete separation of the distributions for 10^{15}- and 2.5×10^{15}-eV primaries. Within the distribution due to primaries of 10^{15} eV it is not generally possible to determine the nature of a primary unambiguously from a knowledge of Δ_c and N. There are two regions where one can do this—all showers with $\Delta_c<15$ were due to copper primaries and all showers with $\Delta_c>1400$ were due to protons. In other regions, one can only give probabilities that a given shower was due to a particular type of primary.

Table IV gives the sea-level mean and median values of N, Δ_c, and the maximum hadron energy striking any one scintillator $[E_H(\max)]$. This last quantity is related to the experimental quantity Δ_{sn}, the maximum number of particles striking any one of the scintillators shielded by 30 cm of lead. Table IV also gives the percentage of showers with single cores. This is done for two different models of the basic nuclear interaction (fireball p_1, and isobar p_4) for protons and for the fireball model for helium ($A=4$), oxygen ($A=16$), and copper ($A=64$) primaries. In all cases the total primary energy was 10^{15} eV.

Perhaps the most important point brought out by Table IV is that these properties are fairly insensitive to the model of the nuclear interaction but are changed greatly by changing the nature of the primary particle. One sees also that increasing the atomic weight of the primary decreases the central electron density, the maximum hadron energy, and the shower size at sea level, and increases the probability of the shower having a multicored structure.

E. Variation of Core Structure with Altitude

The values in Table IV are for sea level (1000 g/cm², to be precise). As one goes up in altitude, the values change considerably. In particular, the proportion of single-cored showers increases. This is shown in detail in Table V.

We can use Table V to compute the fraction of single-cored showers to be expected at sea level and at 750 g/cm² (Mt. Norikura). To do this, we assume (a) that the composition of cosmic radiation is the same at 10^{15} eV total energy as it is at "geomagnetic energies," and (b) that the slopes of the energy spectrum are the same as at these energies.[8] We can compare these predictions with the results of the Sydney 64-scintillator experiment at sea level (Fig. 5) and with those of the Osaka experiment with 48 scintillators of the same size on Mt. Norikura.[7] The Δ_c-N plot of the Osaka group is shown in Fig. 6. There are some obvious similarities between these two distributions. In both cases, the experimental points can be bounded by two lines (labeled p and Fe in the diagrams) which have slopes of unity and intercepts on any ordinate in the ratio 56:1. In both cases, single-cored showers tend to favor the higher values of Δ_c. For instance, on Mt. Norikura the percentage of single-cored showers between the lines labeled p and α is 96%, while between the lines

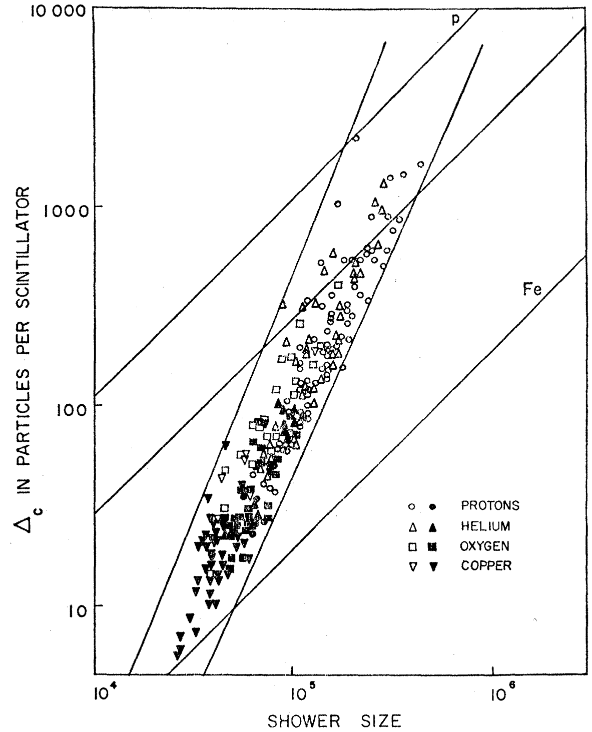

FIG. 4. A plot of the maximum central electron density (Δ_c) at sea level against the total number of charged particles (N) in the shower for simulated showers initiated by 10^{15} eV total energy protons, α particles, oxygen nuclei, and copper, respectively. Open symbols represent single-cored showers, closed symbols are multicored showers. The lines marked p and Fe are the experimental bounds from Fig. 5.

FIG. 5. The experimental distribution of Δ_c and N from the Sydney 64-scintillator experiment. The two steeper lines are the bounds of the simulated distribution for 10^{15}-eV primaries shown in Fig. 4. Open circles represent single-cored showers.

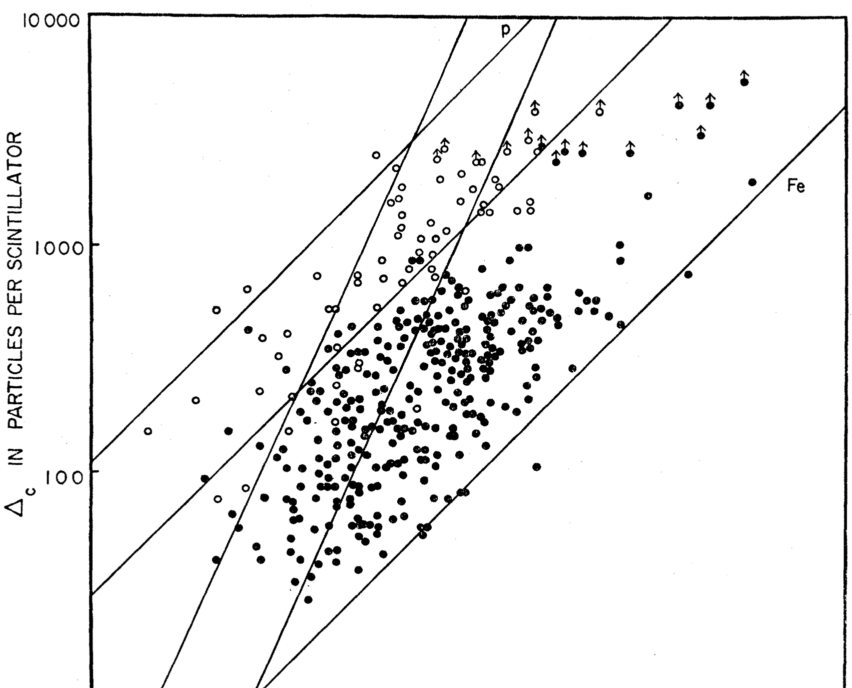

[8] Y. Pal, in *Handbook of Physics* (McGraw-Hill Book Co., New York, to be published).

TABLE IV. Average values and ranges of Δ_c, N, and E_H (max) for shower initiated by different primaries of 10^{15} eV total energy.

Primary	p	p	He	O	Cu
Model	Isobar	Fireball	Fireball	Fireball	Fireball
Δ_c mean	262	318	250	73	29
median	130	175	125	52	21
range	5–2685	23–2300	22–1324	15–406	6–192
$10^{-4}N$ mean	9.5	16.4	13.2	7.3	4.6
median	7.6	15.0	11.5	7.0	4.1
range	1.3–47	5.8–44	4.6–28.9	3.8–17.0	2.6–13
E_H(max) (GeV) mean	12 234	15 697	14 370	4649	1923
median	4267	4013	4840	2597	1020
range	0–122 200	0–235 170	194–236 528	0–34 952	0–12 306
% Single cores	92	69	60	28	11
No. of showers	80	85	50	50	47

labeled O and Fe it falls to 71%. At sea level the respective figures are 80% and 2%. It is also obvious that there is a higher proportion of multicored showers at sea level. To compare with the calculated results we take a slice of the experimental Δ_c-N plots corresponding to a total primary energy of 10^{15} eV. This slice must be taken at shower sizes on Mt. Norikura higher by a factor of 4 as we have seen earlier. The results are given in Table VI. The agreement between the predicted and observed distributions is reasonable, suggesting that at 10^{15} eV the composition of cosmic radiation is the same as at geomagnetic energies.

F. Composition of Cosmic Radiation at 10^{15} and 10^{16} eV

Supporting evidence comes from emulsion observations. In the Sydney 20-liter stack we found 52 protons, 18 α particles, and 42 heavier nuclei of energy greater than 10^{12} eV. The ratio at the same total energy (around 5×10^{10} eV) is 2.2:1:3.2, which is in reasonable agreement with our proportions once we allow for the greater loss of the heavier nuclei in the 6 g/cm² of atmosphere above the flight. At even higher energies, a proton[9] of 2×10^{14} eV, oxygen and calcium nuclei[10] of 2 and 4×10^{14} eV, respectively, and an iron nucleus[11] of 1.2×10^{14} eV have all been observed. It is worth observing that the breakup of a heavy nucleus allows rather good determination of its primary energy.

At energies higher than 10^{15} eV, the situation is different. We have already seen that the change of slope of the number spectrum and its variation with altitude suggest that there is a cutoff in the energy spectrum of at least part of the cosmic radiation at a given energy per nucleon. Since the change in slope comes at around 5×10^5 particles at sea level, we would expect this cutoff to be at ~2–5×10^{15} eV. In Sec. 4 we will see that studies of both the air-shower density spectrum and the high-energy hadron component at sea level confirm this. At the moment, we wish to point out that both the Osaka and Sydney groups have found appreciable numbers of multicored showers of sizes greater than 10^6 particles. In fact, at sea level, the Sydney group (Fig.

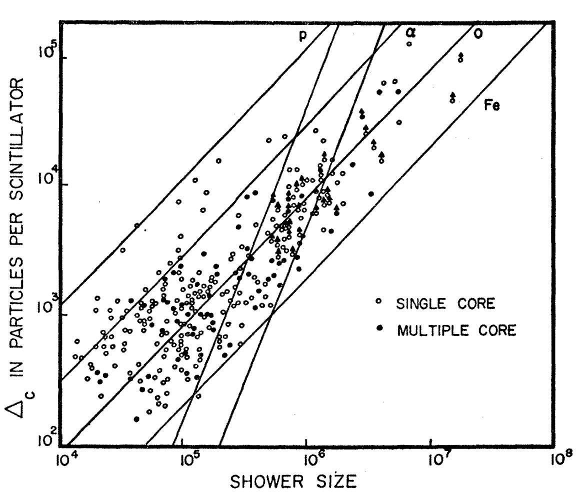

FIG. 6. The experimental distribution of Δ_c against N at Mt. Norikura (Ref. 22).

TABLE V. Percentage of single-cored showers for different primaries (total energy 10^{15} eV) at different atmospheric depths. The same detector sizes were used at all altitudes.

Atmospheric depth (g/cm²) \ Primary	p	α	O	Cu
1000	69%	60%	28%	11%
800	98%	88%	60%	6%
600	100%	100%	90%	38%
400	100%	100%	96%	83%
200	100%	100%	100%	100%

TABLE VI. Predicted and observed values of the fraction of single-cored showers at sea level and at 750 g/cm².

	Predicted	Observed
Sea level	41%	28_{-7}^{+8}%
Mt. Norikura	65%	75_{-8}^{+10}%

[9] J. Kidd (private communication).
[10] M. Koshiba (private communication).
[11] I.C.E.F. Data Book Event 348 (unpublished).

REAL SHOWERS

	22	30			22	202	
	101		45		49	17	
	32	30	18	294	86		22
	382	85	199		475	59	24
81	282	72	Sat	675	38	48	
30	52	62	90	464	323	58	64
46		80	61		30	203	
		13		99	16	10	

SN 16045 $N = 5.1 \times 10^5$

	14			94			
106	516	144	501	10			
41	1037	22	86		22		
	27	8	22				
					11		

SN 20439 $N = 3.4 \times 10^5$

SIMULATED EVENTS

53		85		129			
228					124		
		143	83	249	114	1029	
	100		234	266			
75		1148	563	15411			
123		2433	1184	4437			329
174		1635	3036	117	225	94	205
	220	542	171				701

No. 62 PROTON (p I) 10^{15} eV $N = 1.1 \times 10^5$

			181				780
198							
				403			
56	352	128		86	634		
				1040			
		4148	333		63		
			68	98			

No. 41 PROTON (p I) 10^{15} eV $N = 1.5 \times 10^5$

FIG. 7. Four maps of the distribution of hadron energy on a 4-m×4-m 64-scintillator array. Two are for real showers on the Sydney 64-scintillator experiment. Two are simulated events using 10^{15}-eV proton primaries. All are classed as single-cored showers. For the real showers the energy is represented by the number of particles hitting each scintillator under a 30-cm Pb shield; for the simulated events the actual energy in GeV falling on that scintillator is given. "Sat" means that the scintillator is saturated ($\gtrsim 4000$ particles per scintillator). A blank space means that no particles hit the scintillator.

5) find very few single-cored showers of size greater than 10^6. These large multicored showers lead to some very interesting speculations, which are dealt with in the next section. Their preponderance at sea level for $N > 10^6$ implies that the proton component is much reduced in this size region (10^6 to 5×10^7 particles). (Using mode 6 $p3$ and proton primaries of energy 5×10^5, 10^6, and 2×10^6 GeV we get 31%, 50%, and 71% single-cored showers at sea level, respectively. The respective mean sizes were 0.44×10^5, 0.85×10^5, and 2.60×10^5 particles.)

4. HADRON COMPONENT IN AIR SHOWER CORES

A. Hadrons and the Response of Shielded Scintillators

Our program calculated the number and energy of the hadrons falling on each scintillator of the 9×9 array at each of five atmospheric depths. Experimentally, what one can measure is the response of a scintillator shielded by some sufficient amount of material (30 cm of lead in the case of the Sydney experiment). Obviously, then, it is not possible to make such a direct comparison between prediction and experiment as was the case with the electron component. The Sydney group[12] have calculated that the mean number of particles $\langle n \rangle$ observed in a scintillator beneath 30 cm of lead, and the energy E in GeV of an incident hadron are connected by $E = 1.6\langle n \rangle$ GeV.

This was done using a Monte Carlo calculation of the nucleon cascade in lead. Some experimental tests of part of this calculation have been made, but the overall test of seeing a particle of given energy strike the lead and observing the scintillator response has not yet been possible. One must always remember, too, that this refers to the average response and fluctuations may be large. In fact, it is quite possible for an individual hadron to pass through 30 cm of lead without interacting.

In Fig. 7 we show four events which produced typical single-cored showers both in the electron and in

[12] M. M. Winn, R. H. Wand, J. Ulrichs, M. H. Rathgeber, P. C. Poole, D. Nelson, C. B. A. McCusker, D. L. Jauncey, D. F. Crawford, and A. D. Bray, Nuovo Cimento **36**, 701 (1964).

REAL SHOWERS

	12	44					
			85	8			
	18	46					
365			12	453	20		
	23		187	72			
	30						89
	104						

SN 20210 $N=5.5\times10^5$

SIMULATED EVENTS

					120	389	
57				133			
	59		145	121			
			65				

No. 49 (O I) 10^{15}eV $N=5.9\times10^4$

	33				168	248	
			44		120	114	29
	14	Sat		167	131		28
		83	42	1020		78	69
		8	45	32	250	67	
				150	19	27	31
10					11	34	57
	97	36	531				

SN 17436 $N=9.8\times10^5$

		1837			80	426	4114
	241	225	171	553		185	
		154	2374	4347	284		
		143	86	880	1022	66	440
	845		855	819		946	
196		119	178		94		
		167					

No. 48 (O I) 10 eV $N=1.1\times10^5$

FIG. 8. The distribution of hadron energies in four multicored showers. Again, two are real events which hit the Sydney 64-scintillator array and two are simulated events initiated by heavy primaries of 10^{15} eV total energy.

the hadron component. Two of the showers are real events observed with the Sydney 64-scintillator array and two are simulated events. Figure 8 shows four multicored showers; again, two are real and two are simulated. We find that for the hadron component as for the electron component there is a strong tendency for proton primaries to produce single-cored showers, and for copper primaries to produce multicored showers.

We call the maximum hadron energy observed on one scintillator in any shower E_H(max). Table IV gives the mean and median values of E_H(max) at sea level and its range for the different types of primary particle (each of total primary energy 10^{15} eV). Just as for the electron component, $\langle E_H(\max)\rangle$ is not very dependent on the nuclear model chosen for any given primary particle, but does vary considerably in going from proton to copper primaries of the same total energy.

B. Effect of Hadrons on Unshielded Scintillators

Figure 9 shows the mean number of hadrons hitting the central scintillator plotted against the mean Δ_c for five different ranges of Δ_c. This is for the isobar model p_4, using proton primaries. This model gives a higher density of hadrons in the center of the shower than

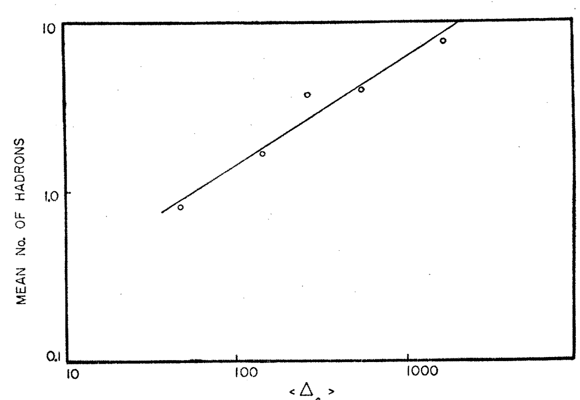

FIG. 9. The mean number of hadrons of energy greater than 50 GeV hitting the central scintillator plotted against the central electron density Δ_c for simulated showers initiated by 10^{15}-eV protons. The isobar model was used.

any other. One sees, for instance, that the mean number of hadrons hitting the central scintillator is six for a central density of 1000 electrons per scintillator. It is of interest to calculate what effect these hadrons could have on the electron density measurement made by the scintillator. Whatever the effect is, it will be an upper limit, since all other scintillators are struck by fewer hadrons. The hadrons which interact can deposit energy in the scintillators in four ways, viz., by produced charged mesons, by evaporation prongs, by knock-on protons (grey tracks), and by the soft cascade from π^0 mesons. In addition to the six hadrons mentioned, we must allow for hadrons whose energy is less than our cutoff of 50 GeV. Details of the computation are given in Appendix A. The result is that the upper limit for the total energy lost in the central scintillator due to hadron interactions is 134 MeV, which is the equivalent of 6–7 particles at minimum ionization, an increase of 0.6% in Δ_c. For other scintillators within 2 m of the core, the value is much lower (23 MeV). Thus the suggestion of the Kiel group,[13] that the multiple cores which they and other groups observe are due to local nuclear interactions in scintillators or in their material above the detectors, is untenable.

C. Hadron Energy and the Electron Density Spectrum

The maximum hadron energy varies rapidly with altitude. Figure 10 shows the median value of the maximum hadron energy plotted against depth in the atmosphere. The same figure also shows the median

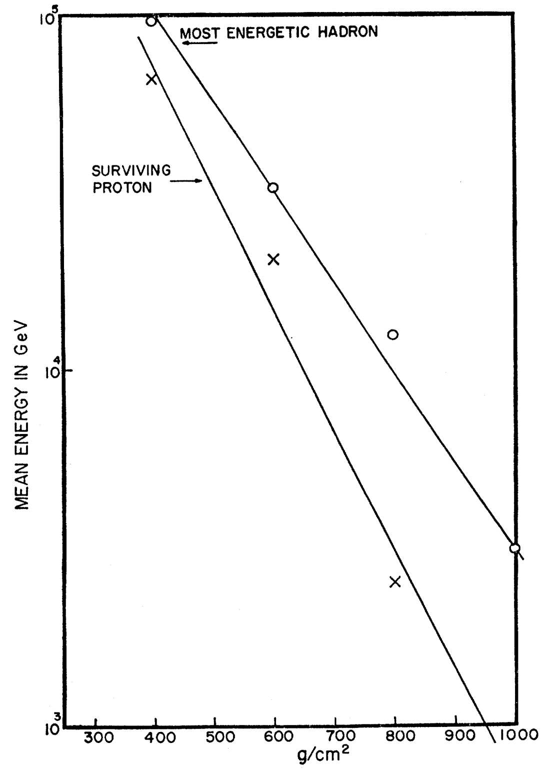

FIG. 10. A graph of the average value of the maximum hadron energy at a given atmospheric depth plotted against atmospheric depth for simulated showers using proton primaries of 10^{15} eV. The mean energy of the surviving proton primary is also shown.

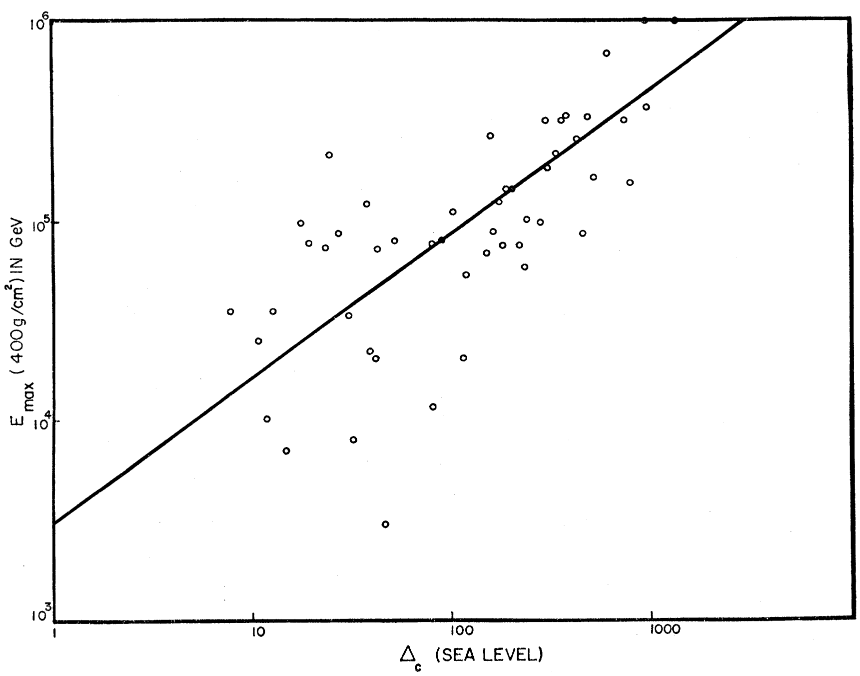

FIG. 11. The scatter diagram of the maximum hadron energy at 400 g/cm² [$E_{\max}(400)$] against the central electron density at sea level (Δ_c) for 50 simulated showers initiated by 10^{15}-eV proton. The line is for $E_{\max}(400)=3000\Delta_c^{0.72}$ GeV.

[13] E. Bohm, W. Buscher, R. Fritze, V. J. Roose, M. Samorski, R. Staubert, and J. Trümper, Can. J. Phys. 46, 41 (1968).

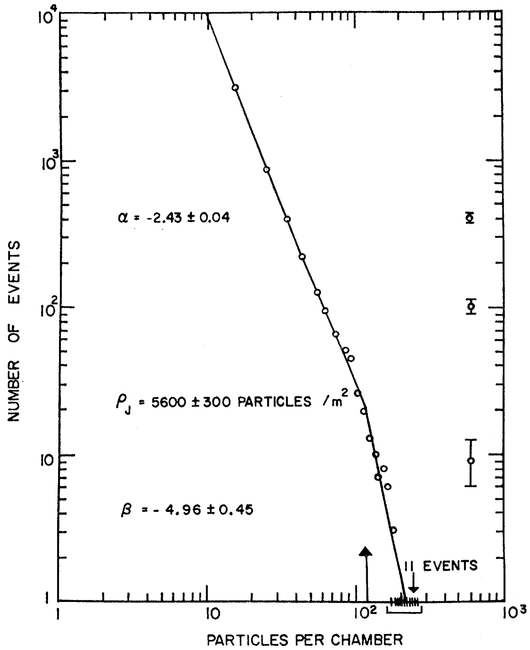

FIG. 12. The density spectrum of extensive air showers determined on Sulphur Mountain, Alberta (781 g/cm²). The solid curve is for two power laws of exponents α and β, respectively, joining at a density $\rho_J = 5600$ particles/m².

value of the energy of the surviving proton primary. It is worth noting that if we take the mean elasticity to be 0.5 (which is what we put into the calculation), then the interaction mean free path of the protons comes out as 90 g/cm² (which is a check on the accuracy of the calculation since that also is what we put in). However, the maximum hadron energy falls off more slowly. The way in which E_H(max) falls off with altitude is of great interest experimentally. It is this quantity which controls the maximum energy of neutral pions at a given altitude. This in turn controls the maximum observed electron density at lower altitudes. This is shown in Fig. 11, where we plot a scatter diagram of E_H(max) at 400 g/cm² against Δ_e, the maximum electron density at sea level. Again this is for proton primaries, using the isobar model. For other primary particles the fluctuations are much smaller. For protons, the two quantities are related by

$$E_H(\text{max}, 400) = 3000[\Delta_e(\text{sea level})]^{0.72}\ \text{GeV}.$$

The determination of the density spectrum of air showers is a much easier experiment than the determination of the number spectrum. For the number spectrum one can only sample the number of particles, and generally the extrapolation factor from sample to number is of the order of 10^6. Moreover, a structure function must be assumed. For the density spectrum the measurement of the number of particles hitting a small area can be exact. The experiment can be (and has been) done at differing altitudes with the same apparatus, the spectrum itself can be representedal most exactly by a simple power law over a range of density of at least 500 to 1, and when the change in slope does appear it is quite rapid. The density spectrum obtained by the Sydney and Calgary[14,15] groups on Sulphur Mountain (781 g/cm²) is shown in Fig. 12. It can be seen from the figure that the differential spectrum at that altitude is quite closely approximated by two power laws of slopes -2.43 ± 0.04 and -4.96 ± 0.45 joining at a density of 5600 ± 300 particles/m². At sea level the spectrum has a similar shape but the join point comes at a much lower density (560 ± 180 particles/m²). Figure 13 shows the way in which the density at the join point of the two power laws varies with altitude.

It was first pointed out by Norman[16] that the change in slope of the density spectrum could be due to a cutoff in the primary energy per nucleon spectrum. If this is so, then one expects the density at which the spectrum steepens to increase rapidly with altitude, so that Fig. 13 is experimental confirmation of Norman's hypothesis.

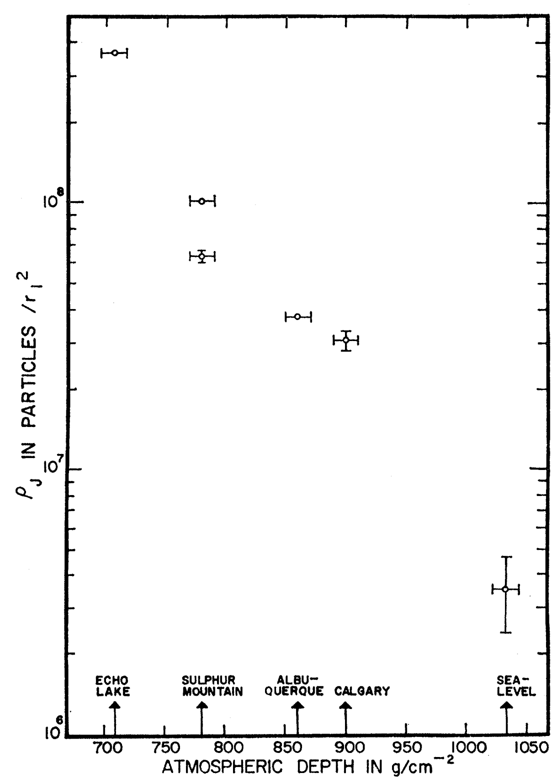

FIG. 13. The variation of the join-point density of the density spectrum with altitude. The join-point density is obtained by finding the best three-parameter fit to the experimental density spectrum at each altitude.

[14] J. B. T. McCaughan, C. B. A. McCusker, S. H. Seet, R. H. Wand, B. O'Donnell, J. D. Prescott, and B. G. Wilson, Nuovo Cimento **38**, 697 (1965).

[15] D. B. Swinson and J. R. Prescott, Can. J. Phys. **46**, 292 (1968).

[16] R. J. Norman, Proc. Phys. Soc. (London) **A69**, 803 (1956).

We can use the results of our Monte Carlo calculations to estimate the energy at which the cutoff occurs. We have seen that $E_H(\text{max},400) = 3000\Delta_c^{0.72}$ (sea level). Putting in the experimentally determined join point of the density spectrum at sea level, we get a corresponding maximum hadron energy at 400 g/cm^2 of $(8\pm2.6)\times10^{13}$ eV. Assuming an inelasticity of 0.5 in nucleon-air nucleus collisions and an interaction mean free path of 80 g/cm^2, we get a corresponding primary energy at the top of the atmosphere of $(2.6\pm0.8)\times10^{15}$ eV. This should be compared with the value of 2 to 5×10^{15} eV, which we obtained from the number spectrum. (When we started these computations some years ago, 90 g/cm^2 seemed the most reasonable value of the proton interaction mean free path and for purposes of comparison we have continued to use this in the Monte Carlo calculations. Experimentally, 80 g/cm^2 now seems better.)

D. Possible Method of Primary Composition Analysis

In Appendix B we give the values of Δ_c, N and Δ_{sh} for the 124 real showers recorded by the Sydney 64-scintillator array which lie in the same region of the Δ_c-N plot as the simulated showers due to primary

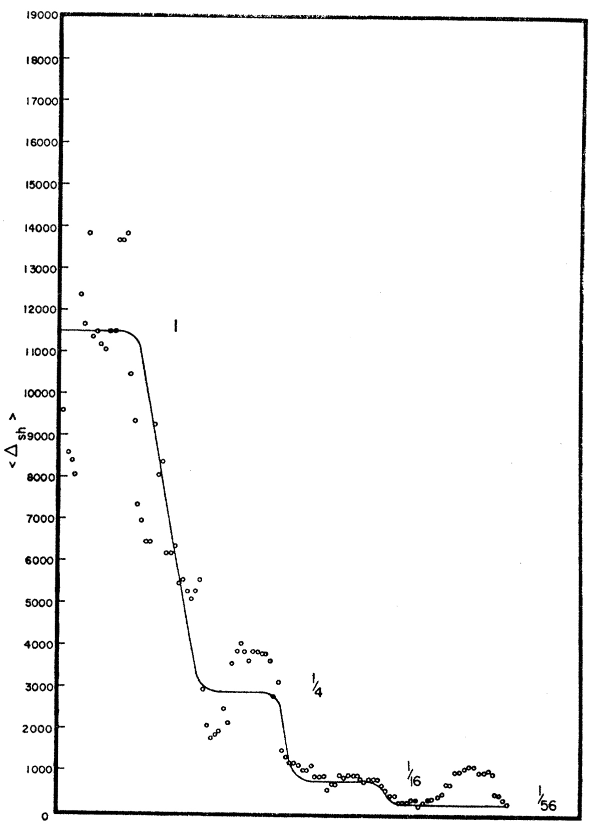

FIG. 14. A graph of the running mean of the maximum hadron energy for twelve consecutive showers from the list of experimental showers given in Appendix B. The stepped curve is the behavior expected if fluctuations were negligible and the primary composition similar to that at 10^{11} eV total energy.

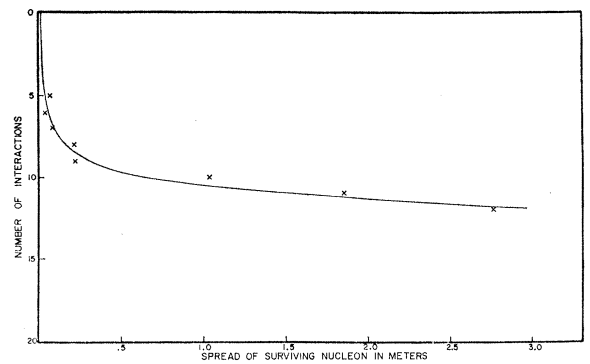

FIG. 15. The mean spread of the primary proton from the shower axis plotted against the number of nuclear interactions it has suffered.

particles of 10^{15} eV total energy. For comparison we also give 124 simulated showers chosen at random from a set of our simulated events weighted to have the same primary composition as at 5×10^{10} eV total energy. Both sets of showers have been arranged in order of decreasing Δ_c. The similarities between the two lists are obvious. One can also see that it would be impossible to duplicate the experimental list if we used simulated showers from only one type of primary.

Another feature of the two lists is that, by arranging them in order of Δ_c (the maximum electron density), we have, also to a close approximation, ordered them in order of Δ_{sh} (the maximum shielded density) or, for the simulated showers, $E_H(\text{max})$. The mean Δ_{sh} for the first 12 real showers is 961; for the last 12 it is 18.4, a ratio of 52:1. These numbers are approximations to the average maximum hadron energy remaining at sea level in two sets of showers of the same total primary energy. If the first set were produced by proton primaries and the second set by iron primaries, the expected ratio would be 56:1. This method could obviously be extended, if we had a large enough sample, to determine the composition of cosmic radiation at a given high energy. In Fig. 14 we plot the running mean of Δ_{sh} for a sample of 12 real showers from the list of Appendix B, starting with the mean of 26068, through 30259. The two ends of the curve are obviously badly affected by fluctuations. At the upper end this is probably due to the inherently large fluctuations in proton showers. At the lower end, it is upset by the low energy cutoff of the apparatus. Nevertheless, it is possible to imagine that the stepped curve, with steps of the ratio of $1:\frac{1}{4}:\frac{1}{16}:1/56$, is a good fit. The steps, of course, correspond to the ratios of energies per nucleon for protons, α particles, oxygen nuclei, and iron nuclei of the same total energy. In a large sample the width of the steps would give the fractions of each component in the primary beam.

E. Lateral Spread of Surviving Nucleons

Suppose we define the axis of the shower as the direction of the primary particle before it hit the atmosphere,

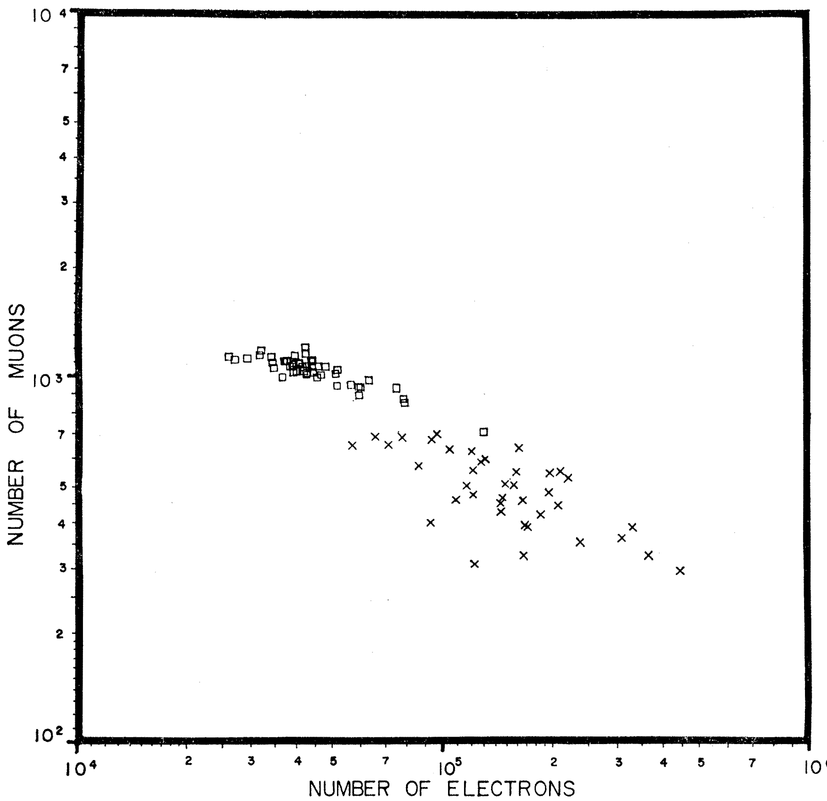

FIG. 16. The scatter diagram of the number of muons (N_μ) in a shower at sea level plotted against the number of electrons (N_e) for showers produced by proton and copper primaries, each of total energy 10^{15} eV. Crosses represent proton showers.

prolonged. Then, as any nucleon cascades down the atmosphere it will wander away from the axis. In our simulations using the isobar model we "tagged" the primary proton. Figure 15 shows the mean distance from the axis in meters of the primary proton (using model p_5) after a given number of collisions. After nine collisions, the spread increases very rapidly. For a primary iron nucleus of the same total energy, this rapid increase in spread would occur five or six collisions earlier, since the energy per nucleon starts out 56 times less and $1/56=K^{5.8}$ if $K=0.5$.

Model p_5 was similar to p_4 except that we tried a high mean transverse momentum for fireball and isobar $[\langle p_T\rangle=4$ GeV/$c]$. This rapid increase of the spread of the nucleons as they go down the atmosphere is important when comparing results with different apparatus at different altitudes, e.g., the BASJE array at 520 g/cm^2 with 2-m×2-m scintillators, and the Sydney array at 1030 g/cm^2 with 0.5-m×0.5-m scintillators.

5. MUON COMPONENT IN AIR SHOWERS

A. Number of Muons in Showers

The scatter diagram of N_μ against N, the total number of particles in the shower for both proton and copper primaries, is given in Fig. 16. The much greater fluctuations for proton primaries than for copper primaries is obvious. In fact, for copper primaries, N_μ fluctuates only within narrow limits—it is almost a characteristic of a particular primary energy.

B. Lateral Distribution of Muons

Figure 17 shows the average lateral distribution of muons of energy >50 GeV in the showers. The curves labeled p and Cu are for simulated showers having, respectively, proton and copper primaries of total energy 10^{15} eV. In both cases we were using the fireball model with a mean transverse momentum of the secondary π mesons of 0.5 GeV/c. The dashed curve is the experimental result of Earnshaw *et al.*[17] for rather large showers (mean size 2×10^7 particles) which we have converted to a mean size of 1.5×10^5 particles, using their experimental law

$$N_\mu \propto N^{0.77}.$$

It can be seen that the agreement is not good. In both simulated cases, the falloff in muon density with radius is much too rapid. This suggests that there may

[17] J. C. Earnshaw, K. J. Orford, G. D. Rochester, A. J. Somagyi, K. E. Turver, and A. B. Walton, Proc. Phys. Soc. (London) **90**, 91 (1967).

TABLE VII. Values of rP_L/h in GeV/c for 10 randomly selected simulated showers due to copper primaries. Δ_{c1} and Δ_{c2} are the highest and next highest number of electrons hitting the scintillator. Their corrected values are corrected for the background electron flux.

Cascade No.	$10^{-5}\times$Size	Observed Δ_{c1}	Δ_{c2}	Corrected Δ_{c1}	Δ_{c2}	Separation in meters	rP_L/h in GeV/c
1	0.47	66	25	53	12	2.0	0.77
4	0.39	28	21	22	15	2.2	0.72
9	0.77	50	35	30	15	2.0	0.60
11	0.37	7	7	5	5	3.4	0.51
12	0.41	21	17	16	12	2.5	0.72
17	0.42	12	10	6	4	1.7	0.33
27	0.44	17	13	11	7	2.5	0.51
32	0.55	42	26	31	15	2.2	0.84
35	0.37	36	26	25	15	2.1	0.67
42	0.73	83	65	45	25	0.7	0.45

be some process operating at high energies which gives average transverse momenta to the produced particles much larger than 0.5 GeV/c.

6. TRANSVERSE MOMENTUM PRODUCED IN VERY-HIGH-ENERGY COLLISIONS

Many experiments have shown multicored structures in the cores of extensive air showers[18–25].

It has been suggested by many of these workers that this demonstrated the existence of processes producing transverse momenta much larger than 0.5 GeV/c, the normal value at accelerator energies. However, before this idea is considered seriously it needs to be shown by adequate Monte Carlo simulation that the same effects could not be produced by heavy primary showers using the normal transverse momenta.

Figures 3 and 4 show that in the simulated showers copper primaries commonly generate multicored showers at sea level. For a total primary energy of 10^{15} eV, the central electron density can be as high as 65 and the separation of the peaks up to 3 m. However, in the experimental results[20–22] peaks with similar separations and very much higher central densities are observed. If we attempt to increase our simulated central density either by using a higher primary energy or by going to a higher altitude (see Table V), we find that the separate peaks coalesce onto one scintillator and we observe a single-cored shower.

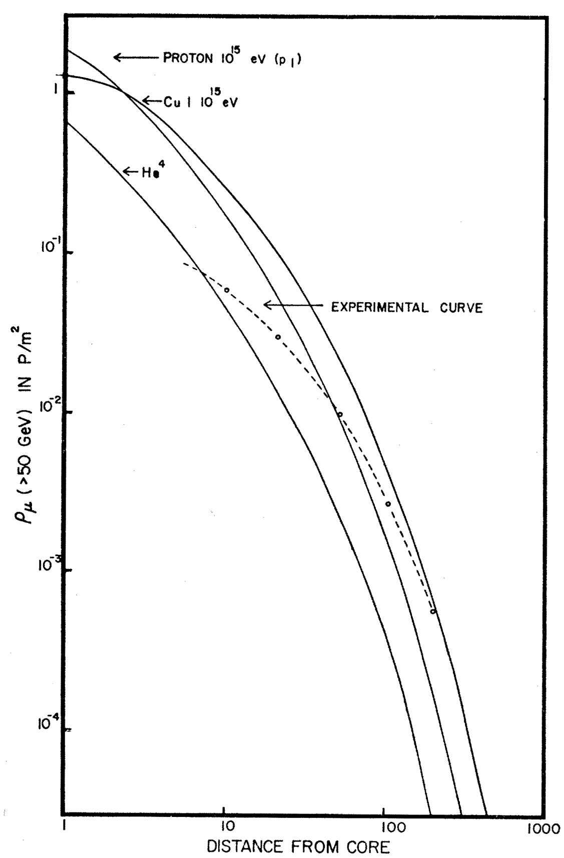

FIG. 17. The average lateral distribution of muons of energy greater than 50 GeV (P=particles) in simulated showers initiated by different types of primary and various assumptions about the transverse momentum. The experimental curve from Ref. 17 is also shown.

[18] R. E. Heinemann and W. E. Hazen, Phys. Rev. **90**, 496 (1953).

[19] N. N. Gorgunov, A. D. Erlykin, G. T. Zatsepin, and A. G. Kannev, in *Proceedings of the Moscow Cosmic-Ray Conference, 1959* (International Union of Pure and Applied Physics, Moscow, 1960), Vol. 2, p. 70.

[20] A. D. Bray, D. F. Crawford, D. L. Jauncey, C. B. A. McCusker, P. C. Poole, M. H. Rathgeber, J. Ulrichs, R. H. Wand, M. M. Winn, and A. Ueda, Nuovo Cimento **32**, 827 (1964).

[21] M. Oda and Y. Tanaka, J. Phys. Soc. Japan **17**, Suppl. AIII (1962).

[22] S. Miyake, K. Hinotani, M. Ito, S. Kino, H. Sasaki, H. Yoshii, H. Sakuyama, and E. Kato, Can. J. Phys. **46**, 25 (1968).

[23] E. Bagge, E. Bohm, R. Fritze, V. J. Roose, M. Samorski, C. Schnier, R. Staubert, K. O. Thielheim, J. Trümper, L. Wiedecke, and W. Wolter, in *Proceedings of the Ninth International Conference on Cosmic Rays, London, 1965* (The Institute of Physics and The Physical Society, London, 1966), Vol. 2, p. 741.

[24] Japanese and Brazilian Emulsion Group, Can. J. Phys. **46**, 660 (1968).

[25] K. Kamata, M. LaPointe, J. Gaebler, I. Escobar, S. Shibata, O. Saavedra, A. Alarcon, K. Suga, K. Murakami, and Y. Toyoda, Can. J. Phys. **46**, 63 (1968).

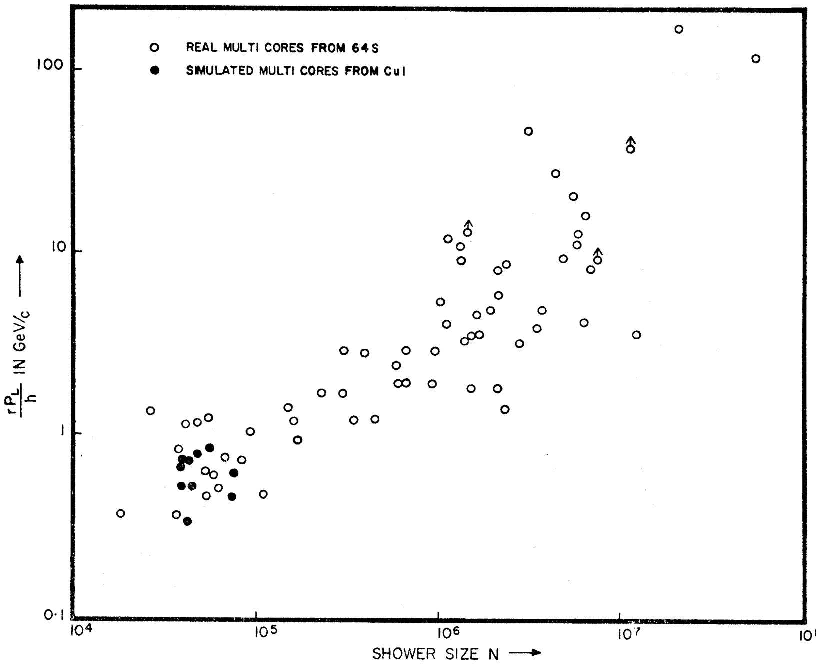

FIG. 18. A plot of the quantity rP_L/h in GeV/c for all multicored showers with $N > 10^6$ observed in the Sydney 64-scintillator experiment together with a random selection of multicored showers from the same experiment with $N < 10^6$ particles. The solid circles are for simulated showers using 10^{15}-eV copper primaries and a mean transverse momemtnum of 0.5 GeV/c.

It appears, then, that to get the well-separated peaks of high central density observed experimentally, we must try a much higher transverse momentum either throughout the cascade or at the higher energies. We first tried the effect of this for proton primaries using the isobar model. This model (called p_5) was identical with p_4 except that the isobar was given a mean transverse momentum throughout the cascade of 4 GeV/c. We found that this large increase produced no effect on the nature of the shower cores. At all altitudes the fraction of single-cored showers was almost or entirely 100%. It seems, then, that to get the effect one requires not only a high transverse momentum but also a heavy primary. One still has a choice between a constant high transverse momentum and one that is high only at high energies.

There is some crude experimental guidance to this choice. From the central electron density of the separate peaks in a multicored shower, one can estimate the height of production h and the energy (hence the longitudinal momentum P_L) of the pions responsible for the cascades. The separation $2r$ of the separate peaks can be directly measured. The quantity rP_L/h then has the dimensions of momentum and, if the pions had both been produced in the one interaction, would be close to their transverse momentum. If the pions come from interactions of different surviving nucleons of the parent nucleus, then rP_L/h will be a rough mean

SIMULATED EVENTS

30	34	37	39	40	38	34	32
37	43	49	53	55	49	42	36
46	58	67	81	96	71	50	40
60	90	97	119	323	97	55	41
72	231	148	102	113	79	52	40
61	97	94	76	68	56	44	36
46	58	73	64	51	44	37	32
36	42	50	48	41	35	31	28

30	36	41	44	45	46	47	37
35	45	56	64	61	61	80	46
39	54	87	118	93	71	62	71
41	61	115	369	127	84	70	68
40	56	86	123	110	108	92	64
36	47	62	78	103	314	175	71
32	39	49	61	86	141	126	64
28	33	40	49	70	69	63	54

FIG. 19. The electron distribution maps at a depth of 600 g/cm² in the atmosphere of two simulated showers initiated by α-particle primaries of 10^{15} eV total energy, using a model in which the mean transverse momentum increased linearly above 10^{14} eV.

of the transverse momenta from the top of the atmosphere down to the point of production of the pions. We can check this statement by carrying out a determination of rP_L/h for simulated showers having copper primaries, where we know that the mean transverse momentum is 0.5 GeV/c. The results are shown in Table VII.

The mean value of rP_L/h is 0.61 GeV, close to the value (0.5) of the mean transverse momentum per interaction put into the simulation.

When the same procedure is applied to real showers, we get the results shown in Fig. 18. All multicored showers of size $>10^6$ particles are shown. Because the number of showers with size $<10^6$ is very large, we have only included a random selection of those events. The simulated showers of Table VII are shown as solid circles. For the real showers Δ_{c1} and Δ_{c2} have been corrected not only for background but also for the "scintillator-to-Geiger" ratio.[26] It can be seen that for shower sizes less than 10^5 particles (i.e., for total primary energies less than about 10^{15} eV) the real showers have values of rP_L/h, very similar to those of simulated showers using a mean transverse momentum of 0.5 GeV/c. For real showers of size greater than 10^5 particles, rP_L/h increases almost linearly with the primary energy. Since we believe we are dealing with showers due to heavy primaries (with A going from 4 through 56) it seems that this increase in transverse momentum is setting in at an energy per nucleon between 10^{13} and 10^{14} eV.

To check this we have used an isobar model, with helium primaries of 10^{15} eV and with a transverse momentum for the isobar constant up to 10^{14} eV, then increasing linearly with energy (we call this model He4). Figure 19 shows two multicored showers resulting from this simulation. It can be seen that this model can produce multicored showers with fairly high central densities.

7. COMPARISON WITH OTHER WORK

A Monte Carlo simulation, almost identical in method to our own, has been carried out by Bradt and Rappaport.[27]The main differences are that it was smaller in scope and designed to simulate the effect on the well-known BASJE array on Mt. Chacaltaya. They used three different nuclear models, two different primary particles (proton and iron), and sampled at two altitudes, 530 and 970 g/cm^2. Where the two simulations can be compared, there is excellent agreement. Both find that for proton showers N_e can vary by a factor of 30:1 at sea level; both find that fluctuations for heavy primaries are much less than for protons; both find that the effects of changing the primary from proton to iron are much greater than those of changing the nuclear model for proton primaries; and both find that the normal "machine" distribution of transverse momenta is in disagreement with several experimental observations.

The calculations of De Beer *et al.*[28] depend more on analytic methods and less on the Monte Carlo technique. Also, they were mostly interested in the muon component. Again, however, where the two calculations can be compared, there is good agreement. For instance, they find, as we do, that the number of muons at sea level in a shower due to a heavy nucleus of a given energy is almost a δ function. They also observe that the normal accelerator distribution of transverse momentum produces too few muons of energy >40 GeV at large distances from the axis.

8. CONCLUSIONS

(1) Emulsion results show that up to 2×10^{14} eV elements from hydrogen up to iron are still present in the beam.

(2) This situation continues up to 2×10^{15} eV. This is shown by (a) the constancy of slope of the density and number spectra up to densities and energies corresponding to this energy, (b) the existence of single-cored showers of high central density in the size range 10^5–10^6 particles at sea level (all attempts to simulate such showers using copper primaries have failed), and (c) the existence of multicored showers of sizes around 10^5. Simulated showers using proton primaries always have a large proportion of single-cored showers at sea level.

(3) Between 2×10^{15} eV and 6×10^{16} eV the primary beam loses first its protons and then progressively heavier nuclei. This is shown by (a) the increase in slope of the number and density spectra beyond numbers and densities corresponding to this energy, (b) the way in which their join points change with altitude, and (c) the decrease in the fraction of single-cored showers at sea level for showers of size greater than 10^6 particles.

(4) Processes may occur at energies greater than 10^{13}–10^{14} eV which produce much higher transverse momenta than are seen around 10^{10} eV (0.5 GeV/c). These transverse momenta seem to increase with increasing energy. This is suggested by (a) the occurrence of multicored showers of size greater than 10^6 particles, and the large values of rP_L/h associated with them, (b) the failure of "normal" values of transverse momentum in our simulated showers to produce multicored showers of high central electron density, even using copper primaries, and (c) the failure of our simulated showers to produce the rather flat lateral

[26] A. D. Bray, D. F. Crawford, D. L. Jauncey, C. B. A. McCusker, D. Melley, D. Nelson, P. C. Poole, M. H. Rathgeber, S. H. Seet, J. Ulrichs, R. H. Wand, and M. M. Winn, Rev. Sci. Instr. **36**, 587 (1965).

[27] H. V. Bradt and S. A. Rappaport, Phys. Rev. **164**, 1567 (1967).

[28] J. F. DeBeer, B. Holyoak, J. Wdowczyk, and A. W. Wolfendale, Proc. Phys. Soc. (London) **89**, 567 (1966).

distribution function for muons of energy >50 GeV, which is found experimentally.

ACKNOWLEDGMENTS

We are grateful to Professor H. Messel and our colleagues of the Sydney Air Shower Group and the staff of the Basser Computing Department for their help. We particularly wish to thank Dr. A. Ueda of the University of Kyoto for his assistance.

APPENDIX A: EFFECT OF NUCLEAR INTERACTIONS IN SCINTILLATORS

In estimating the effect of nuclear interactions in the scintillators, and whether these can form subsidiary peaks, one has to consider the following products: (1) relativistic tracks (mostly charged π mesons), (2) π^0 mesons, (3) knockon targets—or grey tracks, and (4) evaporation tracks from the struck nuclei—or black tracks.

(1) *Relativistic tracks.* If one knows the mean number of nuclear active particles of a given energy E which fall on a particular scintillator per shower $[n(E)dE]$, and, in addition, if the multiplicity of nuclear interactions and the mean free path of the particles is known, the effect of the minimum-ionizing tracks can be estimated. The energy $\mathcal{E}$ lost per scintillator per shower is given by

$$\mathcal{E}\text{ (MeV)}=\int_0^\infty\int_0^{10} 20n(E)e^{-\lambda' x}\lambda'\frac{4\cdot 1}{\ln 16}\ln E\left(\frac{10-x}{10}\right)dxdE\,,$$

where $n(E)dE$ is defined above and can be estimated from the Monte Carlo output. (Although this output only tags nuclear active particles of energy >50 GeV, this can be extrapolated to 1GeV—i.e., the point where we have assumed zero multiplicity.) λ' is taken to be 1/90 cm^{-1} for all nuclear active particles (i.e., a mean free path of 90 cm).

The multiplicity dependence on energy is taken to vary logarithmically starting from $n_s=0$ at $E=1$ GeV, and normalized to $n_s=4.1$ at 16 GeV.

The term $20(10-x)/10$ is the energy lost by a minimum-ionizing track starting from a point x cm from the top of the scintillator whose thickness is 10 cm. (A relativistic track loses 20 MeV on passing straight through the scintillator.)

Neglecting any $\sec\theta$ terms due to inclined tracks (we are only interested in the magnitude involved), we find for showers of primary energy 2×10^{15} eV and using model p_4:

Scintillator	$\mathcal{E}$ (MeV)
Central	72
In a region 0–2 m from core	11
2–5 m	1.8
5–10 m	0.4

(2) *π^0 contribution.* Because 10 cm of the scintillator constitutes only about 0.25 radiation length, the effect of any secondary cascades developing from produced π^0 mesons is small. This can be seen as follows.

Energy of initial γ ray in GeV	No. of electrons after 10 cm development in scintillator
0.75	<1
5	<1
40	~1
300	~2

(3) *Grey tracks.* It can be simply shown that the minimum kinetic energy such a target can have is 250 MeV if the inelasticity of a nucleon-nucleon collision is 0.5. Since the slowest tracks have the highest ionization loss, we assume that all tracks produced have kinetic energy$=250$ MeV. A 250-MeV proton has a range in scintillator material of about 60 cm, so that it is safe to assume that very little slowing down occurs. One then obtains for the gray-track contribution.

Scintillator	E_g (MeV)
Central	9.6
0– 2	1.82
2– 5	0.36
5–10	0.096

(4) *Evaporation tracks.* Finally, we must consider the black tracks. To maximize this effect we assume that for any interaction (i.e., with a carbon nucleus) all the 12 nucleons involved are evaporated and each carries 30 MeV which is lost entirely to the scintillator. This gives as the evaporated energy transferred to the scintillator.

Scintillator	E_B (MeV)
Central	52
0– 2	10.3
2– 5	1.9
5–10	0.52

Hence we can sum these effects to gain an idea of the total energy lost per scintillator.

Scintillator	$E_g+E_B+\mathcal{E}$ (MeV)
Central	133.6
0– 2	23.1
2– 5	4.0
5–10	1.05

Thus the maximum one could observe would be between 6–7 "effective tracks"—not nearly enough to explain the observed subsidiary cores of 100 or more particles. This estimate is consistent with the results of the test run of the 64S array with 32 scintillators directly above the remaining 32 (the "meatless sandwich" run).

APPENDIX B: DETAILS OF 124 REAL SHOWERS WHICH STRUCK THE SYDNEY 64-SCINTILLATOR ARRAY AND 124 SIMULATED EVENTS

	Real showers				Primary	Simulated events			
Ser. No.	Δ_c	N	Δ_{sh}	Type	and No.	Δ_c	N	E_H(max)	Type
26068	>2675	3.5	∼2000	S	p4	2262	2.1	235 176	S
33929	>2385	3.3	1265	S	p76	1656	4.4	5337	S
43158	>2335	5.1	175	S	p32	1408	3.1	3958	S
42911	2325	5.2	375	S	α30	1324	2.9	236 528	S
30839	2150	2.2	225	S	p25	1048	1.7	44 542	S
38360	2075	4.2	1805	S	α6	997	2.8	66 320	S
36379	1975	3.4	235	S	p6	873	3.5	7890	S
43297	1785	2.3	>3000	S	p75	786	3.2	10 194	S
28229	1755	4.6	400	S	α17	655	2.7	18 869	S
35233	1595	2.1	355	S	p74	613	3.0	11 427	S
33825	1565	2.1	93	S	p46	602	2.4	69 364	S
30259	1525	4.1	1600	S	p9	592	2.4	18 092	S
42552	1365	2.3	0	S	α16	583	1.6	18 869	S
38563	1245	3.3	296	S	p43	561	2.2	34 662	S
42151	1195	2.3	0	S	p55	557	2.0	10 130	S
40203	1115	2.2	0	S	p69	543	1.8	37 876	S
29390	1065	2.8	>4575	S	p5	542	2.6	53 426	S
40221	1045	3.3	1100	S	p48	535	1.4	25 542	S
42503	928	2.8	>2405	S	α35	503	2.1	21 549	S
40035	905	3.2	565	S	p73	503	1.9	48 866	S
39778	865	2.7	505	M	α22	497	1.4	17 426	S
34928	845	1.9	0	S	α44	482	2.1	36 822	S
28617	845	2.6	0	M	α36	469	2.2	6768	S
33543	795	2.5	2000	S	α41	439	2.0	4869	S
30419	785	3.2	0	S	O3	406	1.7	13 457	S
31463	765	3.2	∼2500	S	p78	369	2.2	5358	S
27997	735	1.9	0	S	p80	367	1.6	15 937	S
30703	695	1.5	173	S	p70	352	2.1	5691	S
28503	695	2.3	1200	S	p47	345	2.4	18 951	M
43087	558	2.6	0	M	p63	342	1.2	1981	S
43326	552	2.9	375	M	α12	328	1.8	8336	S
40169	527	1.8	194	M	α21	320	1.2	15 652	S
43142	523	2.3	0	M	p66	299	1.6	2648	S
32624	515	1.2	0	M	p14	287	1.6	7221	S
28586	505	1.2	2800	S	p23	269	1.9	76 916	S
40127	473	2.7	795	M	O8	266	1.1	1854	S
43250	465	2.2	343	M	α7	226	1.7	15 851	S
43973	453	2.3	309	M	p11	225	1.8	4013	S
42090	450	2.4	0	M	p3	221	2.1	3130	S
40624	439	1.8	296	M	α11	210	0.93	23 519	S
29972	438	1.4	335	M	O23	205	1.5	16 885	S
43381	407	1.2	114	M	α25	198	1.2	4821	S
43022	384	2.4	90	M	p49	194	1.6	1859	S
29240	383	1.8	0	M	p27	193	1.5	5193	S
43633	360	2.3	184	M	α47	191	1.6	15 092	S
28003	357	2.0	400	M	α14	185	1.7	3406	M
42477	348	1.1	0	M	α28	184	1.2	7791	S
43359	336	1.5	0	M	p39	179	1.5	3735	S
30779	335	1.6	47	M	O1	177	1.0	3886	S
42714	331	1.4	402	M	p67	176	1.6	5874	M
29839	312	2.0	98	M	O42	175	0.91	985	S
33818	310	1.9	825	M	α9	170	1.1	13 415	S
26046	303	1.5	0	S	p62	165	1.1	15 411	M
36421	292	1.5	1625	S	p41	162	1.5	1040	S
42139	288	1.2	288	M	O11	162	1.3	4541	M
39596	284	2.1	183	M	p31	159	1.1	1538	S
33049	277	1.3	0	M	p65	157	1.4	2605	S
31659	274	1.6	174	M	p83	151	1.5	4172	S
35386	268	1.2	185	M	p63	142	1.2	1981	S
42970	241	0.93	0	M	α18	137	1.4	11 180	M
26954	240	1.2	0	S	p7	137	1.5	3002	S
42513	229	0.93	324	M	p68	136	1.2	10 563	S
40100	229	1.0	0	M	p56	132	1.3	258	S
38481	222	1.8	0	M	O48	132	1.1	4347	S
29862	221	1.3	335	M	α40	126	1.2	69 640	S
28716	212	0.78	0	S	p60	123	1.2	3160	M
28825	209	1.0	141	M	p36	123	1.1	3694	M
32700	205	1.5	68	M	O2	122	0.83	2052	M
34684	203	1.4	53	M	O33	119	1.1	753	M
34910	200	1.2	94	M	p35	115	1.2	2943	S
34933	197	1.9	0	M	p59	109	0.95	1299	S

APPENDIX B (Continued).

	Real showers				Primary	Simulated events			
Ser. No.	Δ_c	N	Δ_{sh}	Type	and No.	Δ_c	N	E_H(max)	Type
39790	197	1.3	0	M	α37	103	0.87	2917	S
35498	197	1.5	115	M	p81	103	1.2	2774	S
40160	192	1.9	69	M	α33	97	1.1	1283	M
42280	183	0.82	0	M	p79	95	1.1	4510	M
42727	182	1.1	0	M	p28	94	0.95	2403	M
29725	170	1.3	0	M	α29	94	0.91	7393	M
43111	170	1.4	163	M	O31	92	1.1	688	S
40192	164	0.90	127	M	O26	85	0.71	1773	S
36928	161	1.7	300	M	p8	84	1.1	2747	S
41728	157	1.4	0	M	p44	83	1.1	245	S
30726	157	1.6	156	M	O46	82	0.66	7164	M
42791	156	1.2	0	S	α50	80	0.93	1088	M
43383	154	1.2	0	M	α3	76	0.91	2024	M
34689	152	0.77	0	S	p64	76	1.0	4775	M
31236	142	1.6	0	M	O22	75	1.0	3318	M
36958	138	1.0	78	M	O40	73	0.83	8526	M
34995	136	1.4	0	M	O17	71	0.79	1451	S
41700	129	1.2	0	S	O7	70	0.58	34 952	M
42048	127	0.70	0	M	p1	69	0.77	5755	M
33879	126	1.5	0	M	Cu1	66	0.47	169	S
38513	120	1.4	178	M	α5	66	1.1	837	S
27168	116	1.0	0	M	p50	65	0.93	3051	M
41525	116	0.66	0	M	p84	64	0.87	2040	M
43831	116	1.2	0	M	O32	61	0.72	6040	M
32238	109	1.1	0	M	p18	61	0.83	227	S
32254	104	0.85	47	M	p13	60	0.75	1296	M
40719	104	1.4	0	M	Cu6	60	0.60	3939	S
36351	99	1.0	0	M	p2	60	0.95	254	S
43883	95	1.1	28	M	p58	60	0.91	1420	M
43976	92	1.3	92	M	O35	59	0.84	2492	M
36932	89	1.1	0	M	O12	57	0.71	4645	M
32014	87	0.84	279	M	O13	56	0.84	1015	M
27301	87	1.1	0	M	p38	54	0.75	1311	M
43594	86	1.2	40	M	O21	52	0.70	13 655	M
30695	79	0.59	188	M	O9	52	0.74	391	M
41577	78	0.97	0	M	p20	52	0.80	1312	M
28630	77	0.72	475	M	O38	51	0.76	0	M
27819	76	1.1	0	S	Cu9	50	0.77	662	M
35292	75	0.74	0	M	α24	49	0.71	0	S
43847	75	1.2	108	M	O27	47	0.81	4553	M
32608	74	1.2	185	M	p72	46	0.63	5818	M
43071	67	0.78	0	M	Cu28	45	0.45	1715	M
40162	64	0.84	0	M	α10	45	0.77	0	M
42945	61	0.78	0	M	p12	42	0.72	547	M
36370	58	1.1	0	M	Cu32	42	0.55	7412	M
43879	58	0.44	162	M	p71	39	0.79	900	M
39791	56	0.99	0	M	p16	38	0.81	2851	M
34771	51	0.76	24	M	O34	37	0.57	0	M
35429	46	0.52	0	M	O45	37	0.62	65	M
27887	45	0.77	0	M	O50	37	0.61	6363	M
42190	42	0.82	0	M	Cu35	36	0.38	484	M
38412	41	0.59	0	M	Cu40	36	0.61	91	M
35419	33	0.79	35	M	p22	35	0.67	1337	M